J Mater Sci (2010) 45:3023–3029
DOI 10.1007/s10853-010-4306-x

Microstructural evolution during extrusion and ECAP of a spray-deposited Al–Zn–Mg–Cu–Sc–Zr alloy

Z. L. Ning · S. Guo · F. Y. Cao · G. J. Wang · Z. C. Li · J. F. Sun

Received: 1 August 2009 / Accepted: 7 February 2010 / Published online: 24 February 2010

Abstract The microstructural evolution of an Al–Zn–Mg–Cu–Sc–Zr alloy prepared by spray deposition via extrusion and equal-channel angular pressing (ECAP) was investigated in this study. Deformation route A for Al–11.5 wt% Zn–2 wt% Mg–1.5 wt% Cu–0.2 wt% Sc–0.15% Zr super-strength alloy was carried out at 573 K by ECAP. The microstructures of extruded and ECAP samples were investigated by means of Electron Backscatter Diffraction (EBSD), Scanning Electron Microscopy (SEM) and Transmission Electron Microscopy (TEM). A large amount of dislocation tangles were formed inside grains during ECAP, which further evolved into sub-boundaries and high angle grain boundaries. Microstructure analyses showed that the grain size was refined to 800 nm after 8 passes ECAP from earlier 3.5 μm of sprayed and extruded alloy. A few finer $MgZn_2$ and $Al_3(Sc,Zr)$ were dispersed uniformly after ECAP. The textures of 8 passes ECAPed sample were dominated by the strong Cu orientation and relatively weak S orientation.

Introduction

7XXX series Al alloys are indispensable materials for the aviation and aerospace as well as automotive industries due to their high strength and low density [1, 2]. Their properties are further enhanced by increased Zn concentration [3], at the same time, the disadvantages caused by increasing Zn addition for the conventional casting are also obvious, such as coarse grains, enhanced macrosegregation and high hot crack tendency caused by the low cooling speed, resulting in a low product yield and deteriorative mechanical properties [4–6]. The disadvantages mentioned above were avoided effectively by using spray deposition, in which droplets are first atomised from a molten metal stream, quickly cooled by an inert gas, then deposited on a substrate, and finally built up to form a low-porosity deposit with the required shape. The grain size for the sprayed Al–Zn–Mg–Cu–Sc–Zr alloys containing 12–13% Zn is less than 4 μm after extrusion and the tensile strength is more than 800 MPa [7]. Unfortunately, the relative low elongation of 3–9% restricted their use for high Zn-containing Al–Zn–Mg–Cu alloys widely in complex forming [5, 7–9].

Recent studies have demonstrated that substantial grain refinement in Al alloys can be achieved through the introduction of intense plastic deformation via equal-channel angular pressing (ECAP) [10, 11]. During ECAP, the component undergoes a very severe shear deformation without size change. Pressing can be performed repeatedly and the shear stress cumulates. Grain size is further refined with increased ECAP passes and the superplastic deformation can be realised even at low temperature [9, 10] and high strain rate [11–13] (High strain rate superplasticity (HSRSP) defined as superplasticity at strain rates at or above 10^{-2} s^{-1}, and low temperature superplasticity (LTSP) defined as superplasticity at temperatures below 0.5 T_m, where T_m is the absolute melting temperature.) [14].

Ultrafine grain sizes(less than 1 μm) can be formed for Mg and Al alloys via ECAP [15–17]. Most of previous works have been on microstructure evolution of Al–Zn–Mg–Cu alloys during ECAP process, mainly focusing on

Z. L. Ning (✉) · S. Guo · F. Y. Cao · Z. C. Li · J. F. Sun
School of Materials Science and Engineering, Harbin Institute of Technology, 150001 Harbin, China
e-mail: zhiliangning@sina.com

G. J. Wang
Northeast Light Alloy Co., Ltd, 150060 Harbin, China

7050, 7075 and 7475 alloys [18–20]. More recently, Sha et al. [21] investigated systemically the effects of ECAP on the morphology of precipitates in Al–Zn–Mg–Cu (Al-7136 alloy), showing that ECAP changed the orientation of precipitates and this influences the atomic configuration and the interfacial energy at the η/α-Al interfaces. However, very limited attention has been given to the microstructure evolution of the high Zn-containing Al–Zn–Mg–Cu alloys with trace element addition prepared by spray deposition during ECAP.

The addition of minor Sc and Zr to Al alloy can make the alloy have a higher strength level with higher ductility. Strength increment caused by adding minor Sc and Zr is mainly attributed to fine grain strengthening, precipitation strengthening of Al_3(Sc, Zr) and substructure strengthening.

The objective of this study is to investigate microstructural evolution in a sprayed Al–Zn–Mg–Cu–Sc–Zr alloy containing Zn up to 12% during extrusion and ECAP at 573 K.

Experimental procedure

An alloy with an approximate chemical composition of Al–11.5% Zn–2% Mg–1.5% Cu–0.2% Sc–0.15% Zr (wt%) was prepared by spray-deposition. The as-sprayed ingots were solution treated at 673 K for 12 h, followed by densifying and extruding at 673 K with an extrusion ratio of 20:1 at an extrusion speed of 1.5 mm s^{-1}. The extruded ingot with diameter of 15 mm was homogenised at 733 K for 16 h and cooled in the furnace prior to ECAP. Then, the extruded ingot was deformed by ECAP at 573 K through route A, in which the sample was extruded without any rotation of the sample between successive pressings. An isothermal die with a rectangular cross-section of 10×10 mm and a channel angle of 90° was used. The specimens with 10×10 mm^2 cross-section and 100 mm long were cut from extruded billets. The plunger speed is 1 mm s^{-1}. To minimise the friction between specimen and dies, the graphite powder was used as lubricant. The extruded billets were pressed 4, 6 and 8 passes with approximate total accumulated strain of 6.6, 9.9 and 13.2, respectively, calculated according to the equation by Goforth [22].

For TEM analysis, discs with 3 mm in diameter were cut from the as-extruded and ECAP ingots and ground to a thickness of 0.07 mm. The thin foils were then thinned by twin-jet electropolishing. Microstructural observation was carried by PHILIPS TECNAL transmission electron microscope (TEM) operating at 120 kV. For EBSD analysis, the similar discs were electropolished to give a strain-free surface. The misorientations of grain boundaries were determined by a Hitachi S-3000 scanning electronic microscope with an EBSD pattern collection system operating at 20 kV. The resolution of digital image was 640×480 pixels. Four incomplete pole figures, namely {111}, {001}, {011} and {112}, respectively, were measured. Then, the orientation distribution functions (ODFs) were calculated from the experimental pole figures.

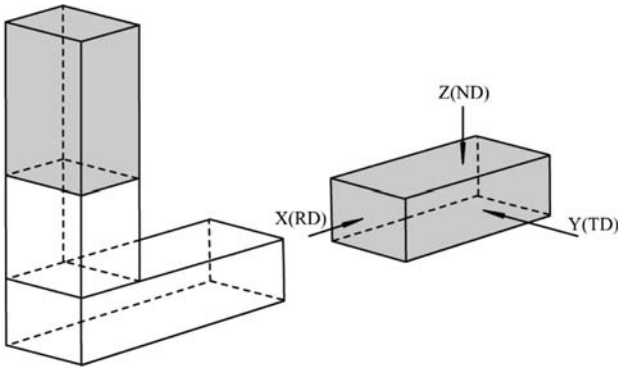

Fig. 1 Schematic illusion of three dimensions and directions observed

Samples for TEM, EBSD and texture measurements were all extracted from the centre of the ECAP processed specimens parallel to both *X* (RD) and *Y* (TD) axis as shown in Fig. 1 in order to avoid the effects of the front and back ends.

Results and discussion

Microstructures of spray-deposited ingot

Figure 2a shows the microstructures of spray-deposited ingot, consisting of equiaxed grains with an particle size of about $20 \pm 3\mu m$. It can be seen that a great number of second phase particles distributed in the spray-deposited ingot. XRD analyses showed that the microstructures were mainly consisted of Al and $MgZn_2$. After solution treatment and extrusion, the finer precipitates were randomly distributed as shown in Fig. 2b. The second phase of $MgZn_2$ existing at boundaries in the as-sprayed samples disappeared. The selected area diffraction patterns (SADPs) of $MgZn_2$ and Al_3(Sc,Zr) were shown in Fig. 2c and d. The EBSD map of as-extrude was shown in Fig. 2e. Black regions represent low-angle boundaries and red regions represent high-angle boundaries. EBSD patterns analysis shows that the deformed zone accounts for 42.69% and recrystallisation zone is 54.67% and the balance is subgrains. The grain size decreases to 3.5 ± 1.2 μm after extrusion.

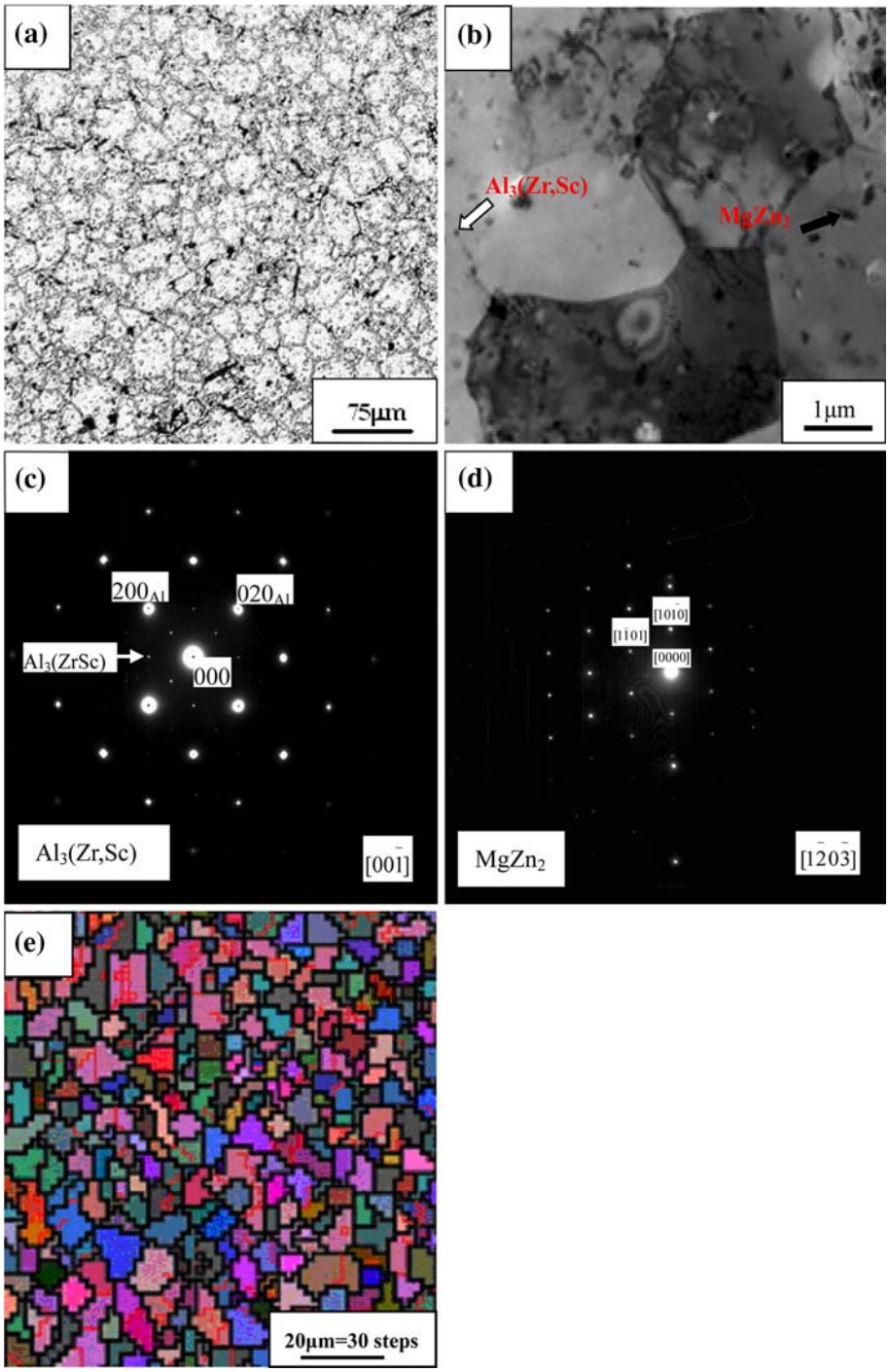

Fig. 2 Microstructures of spray-deposited and extruded Al–11.5% Zn–2% Mg–1.5% Cu–0.2% Sc–0.15% Zr (wt%) alloy at 673 K with a extrusion ratio of 20:1. **a** optical micrograph of as-spray deposition, **b** TEM of as extrusion, **c** SAPD of $Al_3(Zr,Sc)$, **d** SAPD of $MgZn_2$ and **e** SEBD map of as extrusion

Microstructure evolution during ECAP

Microstructural evolution during ECAP by route A was given in Fig. 3. After 4 passes ECAP, the microstructure consisted of two typical structures, one was elongated along shear direction and evolved into band-like structure with length of near 2 μm and width of 1 μm and the other was the nearly equiaxed structure as shown in Fig. 3a. The size of equiaxed grain was about 1.2 ± 0.4 μm. The dislocation distribution was inhomogeneous. A few grains had higher dislocation density distribution, and numerous grains were dislocation free. Transgranular precipitates were partially abated due to the dissolution of second phase particles during severe plastic deformation at higher temperature [23]. Nodular subgrains appeared in the elongated grains. After 6 passes press, most grains exhibited approximately equiaxed structure with a grain size of 1.0 ± 0.2 μm. The difference in grain size was very big and the aligned

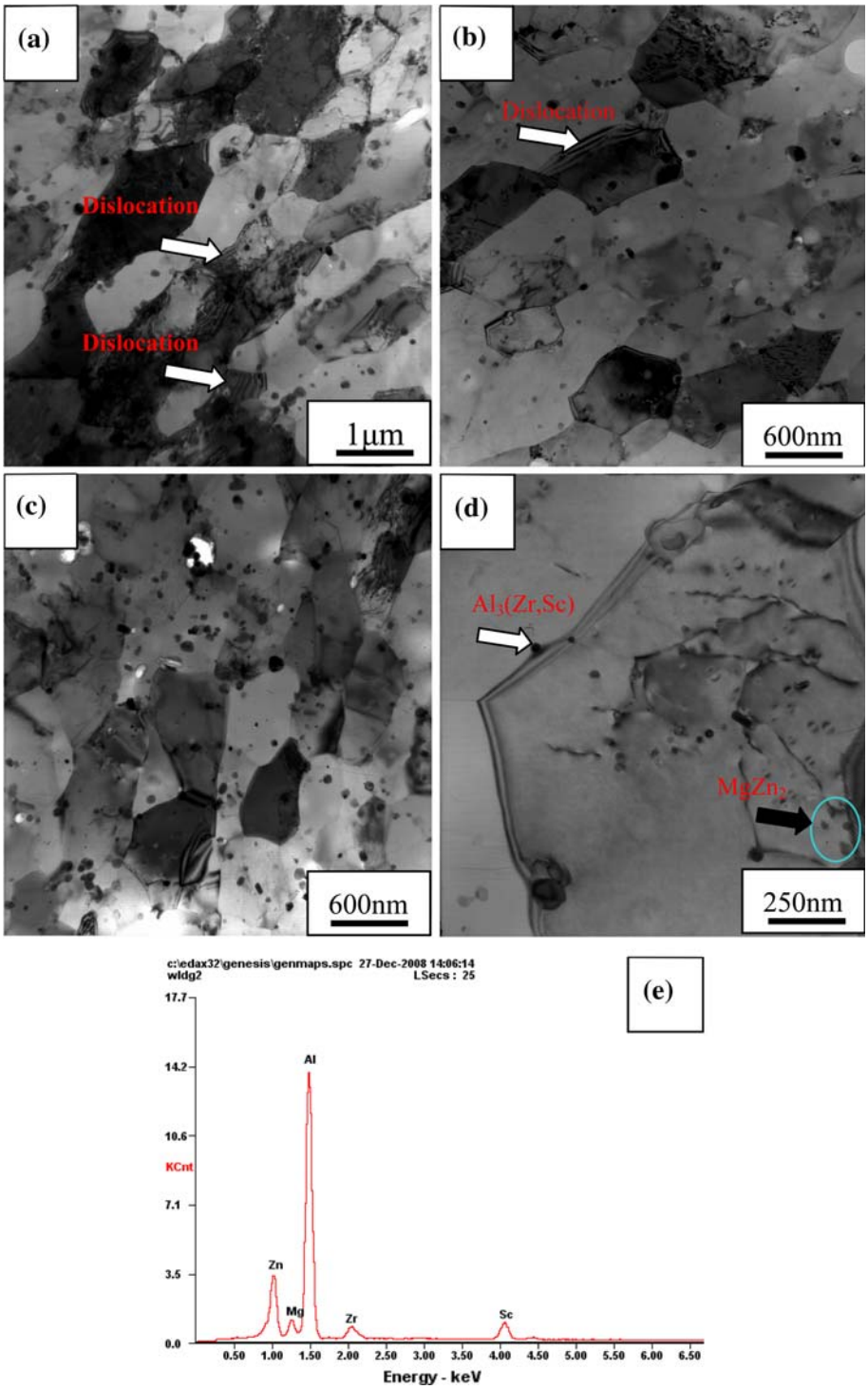

Fig. 3 Typical microstructural evolution during ECAP. **a** 4 passes, **b** 6 passes, **c** 8 passes, **d** magnification of **c**, showing the pinning effect of $Al_3(Zr,Sc)$ particles on the grain boundaries and **e** energy dispersive spectrum of the $Al_3(Zr,Sc)$ particle phase showing high concentration of Al, Zn, Mg, Zr and Sc in the alloy investigated. ECAP at 573 K by route A, observed plane parallel to both *X* (RD) and *Y* (TD) axis as shown in Fig. 1

direction along the press direction was still existed as given in Fig. 3b, indicating that the elongated grains had evolved into the equaixed one. Compared with the microstructure of press with 4 passes, more precipitates were occurred and the finer subgrain boundaries were formed in the subgrains. From 4 passes to 6 passes, the grain size decreased due to an increasing number of equiaxed grains delineated by sharp boundaries and a gradual decreasing of elongated grains. Before 4 passes, there were no precipitates appearing distinctly. Spherical phase precipitates after 6 passes, and the precipitate increases with increased pass to 8. TEM analyse confirm that these precipitates are $MgZn_2$ and $Al_3(Zr,Sc)$ as shown by arrows. The precipitation is promoted by increased ECAP pass at higher temperature.

As the press passes increased to 8 passes, most grains evolved to globular with grain size of 800 ± 200 nm as shown in Fig. 3c. During ECAP at elevated temperature, the supersaturated solid solution decompose, thus precipitating the $MgZn_2$ and $Al_3(Zr,Sc)$ phases. There are a small quantity of rod-shaped $MgZn_2$ precipitates with lengths of 8–30 nm and thickness of 7–15 nm but there were many spherical-shaped precipitates with sizes of 30–50 nm. The rod-shaped $MgZn_2$ phases are formed due to coalescence at high temperature. The spherical-shaped precipitates are probably due to a transformation of the η'-phase into η with subsequent coarsening during ECAP [23]. There are many fine spherical $Al_3(Sc,Zr)$ nanoscale particles precipitated, which effectively pinned the migration of boundaries and sub-boundaries during ECAP as shown in Fig. 3d, inducing the finer structure even ECAPed at higher temperature. The energy dispersive spectrum (EDS) of an $Al_3(Zr,Sr)$ particle corresponding to Fig. 3d is shown in Fig. 3e. At the early stage during ECAP, the coarse grains were elongated along the deformation direction and the some fragmented subgrains with little angle boundary were formed in the initial grains. With the increasing in the deformation, the subgrains continue to deform and form the near globular microstructure with large angle boundary, finishing the change from the subgrain to grain. At the same time, the misorientation angle between grains is also increased with the increased deformation. Compared with the study in Ref. [20], in which the grain size of 0.3 μm was obtained when a spray-cast alloy with the similar chemical compositions without Sc addition was ECAPed (route *Bc*) 8 pass at 473 K, the grain size was 0.8 ± 0.2 μm in the present study after 8 passes. This is attributed to the increased ECAP temperature of 573 K, due to the fact that the average grain size trends to increase with increasing pressing temperature [20, 24].

Typical EBSD map and the distribution of boundary misorientation as well as characteristic microstructure after ECAP are given in Fig. 4. The thick line indicates

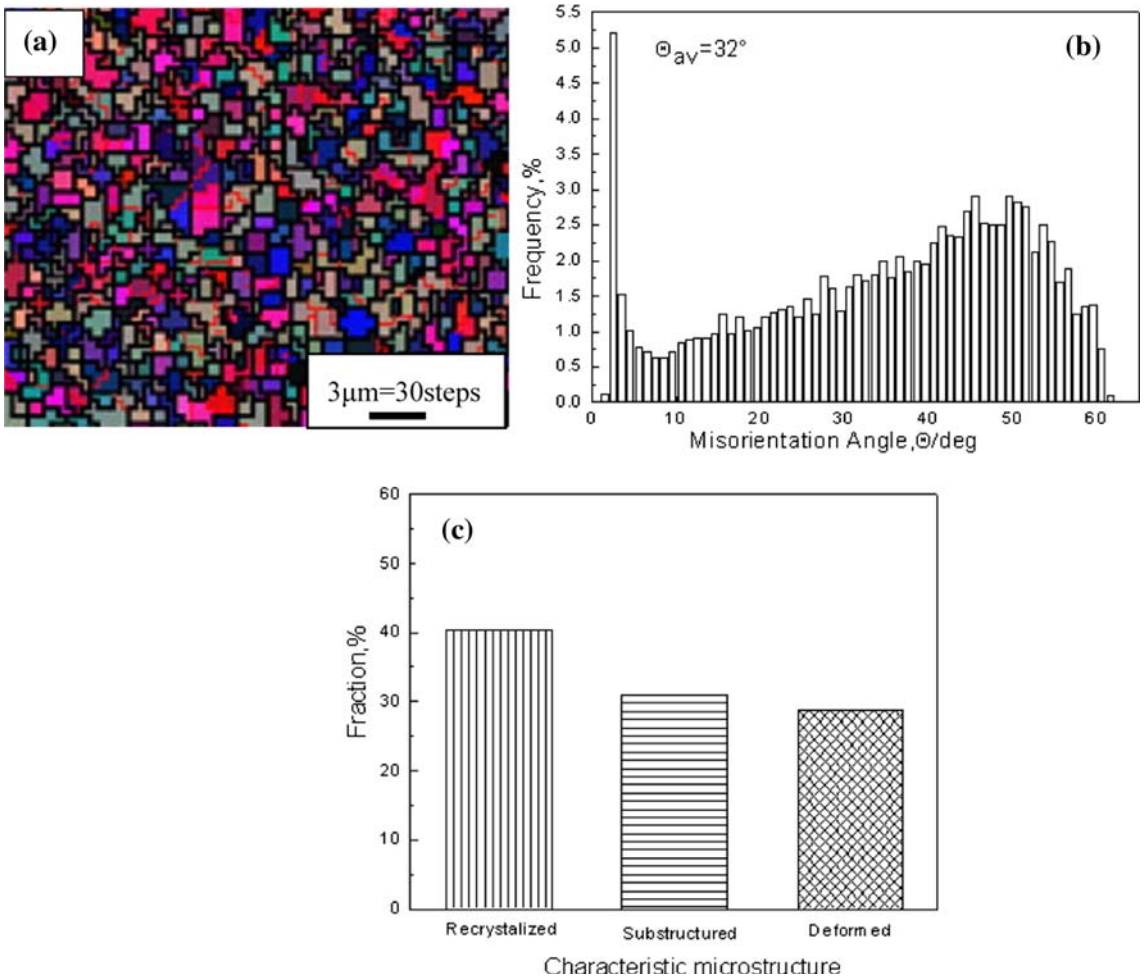

Fig. 4 Typical misorientation distribution. **a** EBSD, **b** misorientation distribution and **c** fraction of grains

high-angle grain boundaries (HAGBs) (≥15°) and the thin line represents low-angle grain boundaries (3°–15°) [15]. During ECAP, a lot of subgrains transit to HAGBs through rotation under severe shear deformation at relative higher temperature, leading to a continuous increase in HAGBs. After 8 passes pressing, the average misorientation is up to 32° and the fraction of HAGBs accounts for 77%. EBSD patterns analysis shows that the deformed zone accounts for 28.76% and recrystallisation zone is 40.26%, and subgrains of 30.98%, showing that a great number of subgrains are formed, which is the benefit for nucleating of recrystallisation. The grain aspect ratio defined as the ratio of the grain dimension in the pressed direction to that in the transverse direction is 1.65. For the comparison, the misorientation angle measurement of extruded sample was also measured to be 28°. After 8 passes ECAP, the misorientation angle increases slight from 28° to 32°. This is likely due to the fact that extruded sample suffered severe plastic deformation with a relatively high extrusion ratio of 20:1, resulting in a high misorientation angle existing in the extruded sample and slight increase after further ECAP. Mobile dislocations move across subgrains and are trapped by sub-boundaries, leading to an increase in their misorientations. As a result, LABs eventually convert to true HABs. This process was clearly illustrated by Kaibyshev et al. [25] in reference.

Microtexture evolution during ECAP

ECAP being an unsymmetrical deformation process, pole figure representation is not sufficient to describe the texture evolution. The corresponding orientation distribution figures are given in Fig. 5. On ECAP, the migration of boundaries during recrystallisation was hindered by nanoscale $Al_3(Sc,Zr)$ dispersoids formed

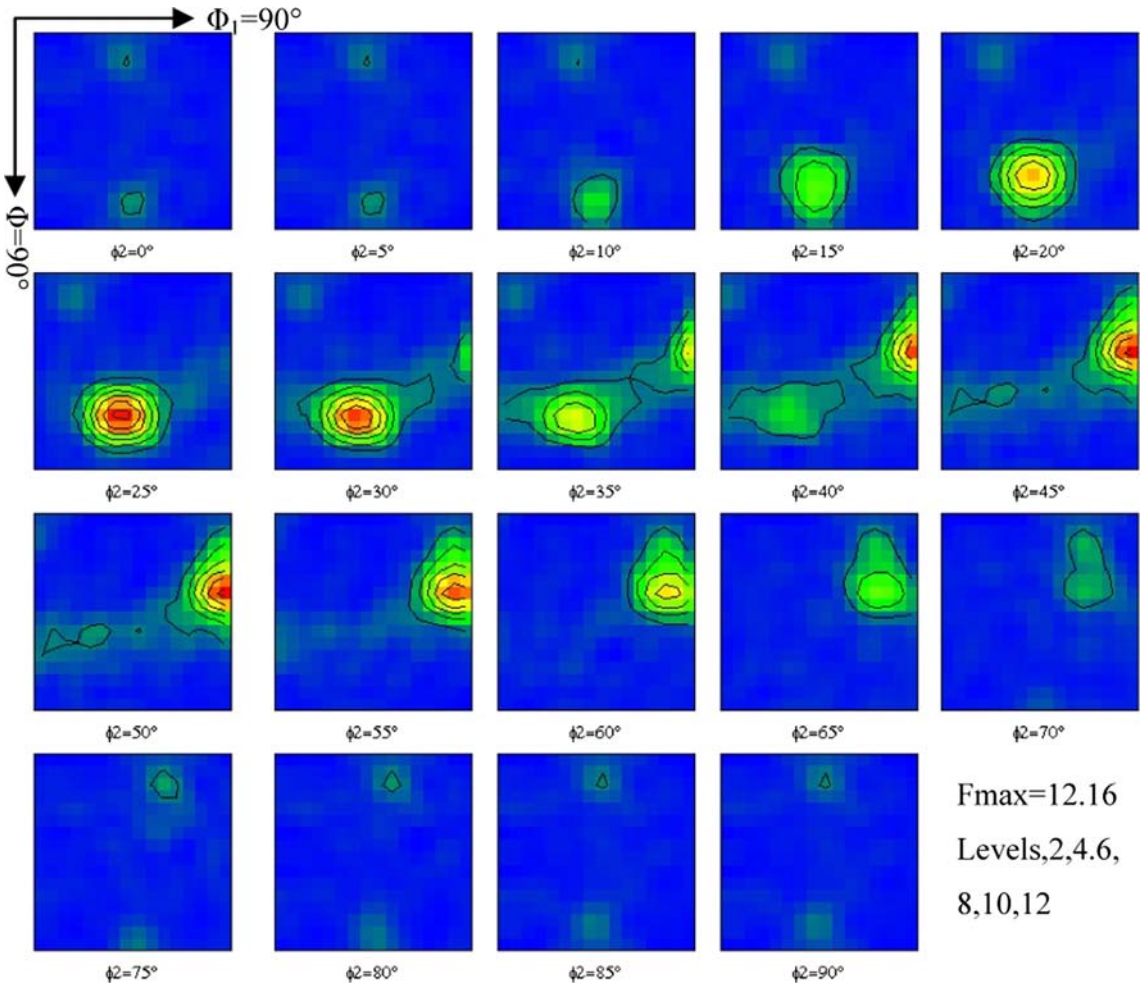

Fig. 5 ODFs for the sample ECAP processed to 8 passes, ECAP at 573 K by route A, observed plane is parallel to both *X* (RD) and *Y* (TD) axis as shown in Fig. 1

both interior (sub)grains and on the boundaries of grains and act as an effective pinning agent to dislocation, leading to a suppression of the formation of cubic texture. With reference to the materials composition, it is known that second-phase particles may strongly affect deformation texture evolution. In most cases, a certain degree of texture weakening is observed, yet more complex effects reported in solid solution on texture evolution is less well-documented [26]. During ECAP, all slip planes have to steer to the shear direction in different level, resulting in a formation of typical copper orientation texture of ($\{112\}\langle 111\rangle$) with maximum intensity of 12.16. The maximum texture intensity was obtained at the 25°, 45° and 50°, respectively. Furthermore, a relatively weak S type texture $\{123\}\langle 634\rangle$ of 4°–5° was observed also, showing that up to maximum strains the textures are dominated by the Cu and S orientations, which is similar with rolled textures [26].

Conclusion

(1) A grain refinement in Al–Zn–Mg–Cu–Sc–Zr alloy containing Zn up to 12% prepared by spray deposition was obtained by ECAP at 573 K after 8 passes pressing with a total strain of 12.16, resulting in a decrease in grain size from 3.5 μm at as-extrusion to 800 nm after ECAP.

(2) After 8 passes pressing, the average misorientation angle is up to 32° and the HAGBs account for 77%. The deformed zone accounts for 28.76%, and recrystallisation zone is 40.26% and subgrains of 30.98%, indicating that a great number of subgrains are formed. The misorientation angle shows a slight increase from 28° as extruded to 32° after ECAP.

(3) After ECAP, the textures are dominated by the Cu orientation with maximum intensity of 12.12 and relatively weak S orientation of 5°–6°.

References

1. Hirsch J, Karhausen KF, Lochte L (2002) Mater Sci Forum 396–402:1721
2. Fridlyander IN (2000) Mater Sci Forum 331–337:921
3. Davis JR (ed) (1993) Aluminium and aluminium alloys. ASM International, Materials Park
4. Grant PS (1995) Prog Mater Sci 39:497
5. De Sanctis M (1991) Mater Sci Eng A 141:103
6. Wang F, Xiong B, Zhang Y (2007) Mater Des 28:1154
7. Yixin W (2008) Micro-alloying and mechanism of Al–Zn–Mg–Cu ultra high strength aluminum alloy prepared by rapid solidification. Dissertation for the Degree of Master in Engineering, Harbin Institute of Technology
8. Hongbin W, Huimin L, Jin-feng H (2004) Chin J Nonferrous Met 14:398
9. Sharma MM, Amateau MF, Eden TJ (2006) Mater Sci Eng A 424:87
10. Vidal V, Zhang ZR, Verlinden B (2008) J Mater Sci 43:7418. doi:10.1007/s10853-008-2746-3
11. Malek P, Turba K, Cieslar M, Dbohlav I, Kruml T (2007) Mater Sci Eng A 462:95
12. Kim WJ, Kim JK, Park TY, Hong SI, Kim DI, Kim YS, Lee JD (2002) Metall Mater Trans 33A:3155
13. Park K-T, Myung S-H, Shin DH, Lee CS (2004) Mater Sci Eng A 371:178
14. Komura S, Furukawa M, Horita Z, Nemoto M, Langdon TG (2001) Mater Sci Eng A 297:111
15. Musin, Kaibyshev R, Motohashi Y, Itoh G (2004) Scripta Mater 50:511
16. Lee S, Furukawa M, Horita Z, Langdon TG (2003) Mater Sci Eng A 342:294
17. Hockauf M, Meyer LW, Nickel D et al (2008) J Mater Sci 43:7409. doi:10.1007/s10853-008-2724-9s
18. Lin HK, Huang JC, Langdon TG (2005) Mater Sci Eng A 402:250
19. Zheng MY, Xue SW, Qiao XG (2008) Mater Sci Eng A 483–484:564
20. Zheng LJ, Li HX, Hashmi MF (2006) J Mater Process Technol 171:100
21. Sha G, Wang YB, Liao XZ, Duan ZC (2009) Acta Mater 57:3123
22. Cabibbo M, Evangelista E, Latini V (2005) J Mater Sci 39:5659. doi:10.1023/B:JMSC.0000040073.78798.d4
23. Zhao YH, Liao XZ, Jin Z (2004) Acta Mater 42:4589
24. Xu C, Furukawa M, Horita Z et al (2005) Acta Mater 53:749
25. Kaibyshev R, Shipilova K, Musin F, Motohashi Y (2005) Mater Sci Eng A 396:341
26. Engler O, Crumbach M, Li S (2005) Acta Mater 53:2241